www.amlett.com, www.vbripress.com/aml, DOI: 10.5185/amlett.2015.5956 Published online by the VBRI Press in 2015

Synthesis and cytogenetic effect of magnetic nanoparticles

Bishnu K. Pandey[1,2*], Ashutosh K. Shahi[2], Nitisha Srivastava[3], Girjesh Kumar[3], Ram Gopal[2]

[1]*Material Research Centre, Indian Institute of Science, Bangalore 560012, India*
[2]*Laser Spectroscopy and Nanomaterial Lab, Department of Physics, University of Allahabad, Allahabad 211002, India*
[3]*Plant Genetics Laboratory, Department of Botany, University of Allahabad, Allahabad 211002, India*

[*]Corresponding author. Tel: (+91) 532-2460764; E-mail: bishnu.pandey750@gmail.com

Received: 12 June 2015, Revised: 26 September 2015 and Accepted: 01 October 2015

ABSTRACT

In the present study we have successfully synthesized cobalt and cobalt oxide NPs in ethanol and double distilled water respectively. Structural and optical characterizations have been performed by X-ray diffraction and UV-Visible absorption spectroscopy respectively. Magnetic characterization has been performed by vibrating sample magnetometer (VSM). Particle shape and size have been estimated by transmission electron microscopy (TEM). We have studied the effect of cobalt and cobalt oxide NPs on mitotic division of meristamatic roots of *Sesbania cannabina*. It has been found that cobalt oxide nanoparticles were more toxic than cobalt nanoparticles and both induced various types of chromosomal aberrations in meristamatic root tip cells of *sesbania cannabina*. Copyright © 2015 VBRI Press.

Keywords: DNA; laser ablation; cobalt nanoparticles; sesbania cannabina; magnetic nanoparticles.

Introduction

Magnetic nanoparticles are of great interest and offer attractive possibilities for researchers in bio-technology, due to the controllable size ranging from few nanometers up to tens of nanometer. Magnetic nanoparticles also provide many exciting opportunity in different field such as, MRI contrast agent; magnetic nanoparticles provide MR contrast enhancement by shortening the both longitudinal and transverse relaxation of surrounding proton [**1-3**]. Hyperthermia of cancer; it is based on the fact that when magnetic nanoparticles are exposed to a varying magnetic field, heat is generated by the magnetic hysteresis loss, Néel-relaxation, and Brown-relaxation [**4**]. Drug delivery; the concept of magnetic targeting is to inject magnetic nanoparticles to which drug molecules are attached, to guide these particles to a chosen site under the localized magnetic field gradients, hold them there until the therapy is complete, and then to remove them [**5**], biotoxin removal [**6**], gene therapy [**7**] and protein purification [**8**]. Recently, ferromagnetic materials have been extensively studied as source of polarized electrons for their possible applications in spintronic devices and quantum computing. A current application of spintronic devices is the use of giant magnetoresistance (GMR) in the read heads of high-speed disk drives. The back bone of DNA is negatively charged, so the binding of magnetic nanoparticles with DNA takes place via electrostatic interaction and causes gene regulation [**9**]. Cobalt oxide is important material that finds applications in different fields such as catalysis, various types of sensors, electrochromic, electrical and other opto-electronic devices. It has been reported that Co_3O_4 is humidity-sensitive in the visible wavelength region at room temperature.

A number of techniques have been used for producing nanoparticles which include gas evaporation, sol–gel methods, sputtering, and co-precipitation [**10**]. Pulsed laser ablation of the solid material in liquid media has attracted much attention over the past few years, and this technique is known as liquid phase pulse laser ablation (LP-PLA), which involves the firing of laser pulses on the surface of solid target immersed into liquid media. In laser pulses, front part of pulse creates vapors on the target surface, which are irradiated by tail part of same pulse. This process causes photo ionization and the generation of dense high-temperature and high pressure laser plasma plume, which expands perpendicular to the target surface into the liquid. This expanding plume interacts with the surrounding liquid particles, creating cavitations bubbles, which upon their collapse, give rise to very high temperature and pressure however these conditions are much localized and on about nanoscale [**11-12**].

Besides it, LP-PLA offers much controlled central parameters to synthesize different size, shape, and nanostructure which can be possible by controlling laser wavelength, pulse width, ablation duration, and laser focusing conditions [**13-14**].

A number of plant bioassay techniques have been developed for the detection of environmental mutagens because plant chromosomes are relatively large and respond to treatment with mutagens in a similar way to mammals and other eukaryotes [**15**]. The testing seed of a green manure crop Sesbania cannabina has been used in the present study since it is fast growing species, commonly known as Dhaincha, Prickly sesban, Sesbania pea etc. *S. cannabina* is a quick growing, succulent, suffructicose, annual leguminous plant and ideally suited as a green manure crop. In India, the species has been introduced as green manure to enhance organic matter in rice fields. *Sesbania* green manuring has substantially improved grain yield, up to 72 % [**16**]. Because of its ability to grow in heavy metal soils and to withstand water logging and tolerate soil salinity, it is often the preferred green manure crop for rice and wheat. It yields a strong useful fibre, durable especially under water. *S. cannabina* shows promises for early fodder and fuel production [**17**]. Here, germinated seeds of *Sesbania cannabina* were treated with cobalt nanoparticles prepared in different media (DDW and ethanol) and its impact on mitotic index and the chromosomal aberration frequencies have been studied. The mitotic index is able to give the percentage of dividing cells in every sample while chromosomal aberration index represent the percentage of aberrant cell divisions. Here we have visualised the different chromosomal distortion.

Experimental

The experimental details for the synthesis of cobalt/cobalt oxide NPs are same as described earlier [**11, 12**]. The slice of thin cobalt rod of high purity (99.99 %) (Spec pure, Johnson Matthey England), was immersed into the liquid media (DDW and ethanol). The slice was ablated by focused output energy of 40 mJ/pulse from pulsed Nd: YAG laser (Spectra Physics- Quanta Ray, U.S.A.) operating at 1064 nm wavelength and 10 Hz. for 0.30 hr. The laser beam was focused into a 0.50 mm spot diameter on the target surface using a lens through 17 mm length of liquid media. The container with target was translated along the length of the rod to avoid the inhomogenity of ablation and crater formation in liquid media. All the experiments were performed at room temperature and at 1 atmosphere pressure. Obtained colloidal solutions of cobalt/ cobalt oxide NPs were stored in plastic containers at room temperature for further shocking of seed. UV-Visible absorption spectra have been recorded using a Perkin Elmer Lambda 35 double beam spectrophotometer of synthesized colloidal NPs, with the corresponding liquid media as a reference. The colloidal solution was dried at 60 ^{o}C for 10 hr in oven. The beam line-12 at Indus-2, Synchrotron radiation source (RRCAT-Indore) has been used for X-Ray diffraction of obtained powder of cobalt oxide NPs. Synchrotron radiation energy was 10.87 KeV, with wave length 1.14084 A. TEM analysis has been performed by using TEM (model number FEI Tecni G2F30STWIN). A drop of colloidal solution of NPs was placed on the copper grid and dried at 60 ^{o}C before imaging the particle shape and size. The magnetic measurement has been carried out by a VSM (ADE-DMS, EV-7, USA) at room temperature.

Procurement of seeds

Seeds of *Sesbania cannabina* variety ND-1 were obtained from Sunn-Hemp Research Station, Pratapgarh, U.P. India.

Treatment and fixation of root meristems

Dry and healthy seeds of Sesbania cannabina were soaked in distilled water for 14 hrs and afterwards kept at room temperature for rooting. After rooting seeds were treated with cobalt, cobalt oxide nanoparticles and ethanol solution for three hours. Control was maintained separately in distilled water. Treated as well as control seeds were fixed in Carnoy's fixative (1:3 glacial acetic acid: absolute alcohol) for 24 hours and afterwards soaked in 90% alcohol. Samples were stored in the refrigerator until they were used for chromosomal aberration assay.

Chromosomal aberration assay

Four different treatment sets (control, ethanol, nano-cobalt and nano-cobalt oxide) were used for the chromosomal aberration assay. For cytological analysis treated as well as control root tips were hydrolyzed in 1N HCl at 60 °C for 5 minutes.

These hydrolysis root tips were thoroughly washed with water several times to remove HCL. Afterwards the root tips were dried between sheets of filter paper to remove excess water and later they were kept in 2 % acetocarmine for staining. After staining the dark stained tip portion of root tips were used for slide preparation.

Scoring of slides

Slides were observed under Nikon microscope (40 X) and AMI and total abnormality percentages were calculated for each treatment and control set. For chromosomal aberration assay slides were scored for chromatid and chromosome aberrations only in metaphase and telophase for each treatment sets and control more than 500 cells were observed.

Formula used,

$$AMI\% = \frac{\text{Total number of dividing cells} \times 100}{\text{Total number of cell observed}}$$

$$\text{Total abnormality } \% = \frac{\text{Total number abnormally dividing cells} \times 100}{\text{Total number of cell observed}}$$

Results and discussion

X-ray diffraction

XRD pattern of cobalt oxide NPs as synthesized by LP-PLA in DDW is shown in **Fig. 1**(**a**). The patterns at 2θ= 26.98^{0} and 32.64^{0} are assigned to Co_3O_4 with plane (311) and (400), (JCPDS Card number 74-2120) with face centered cubic system. The crystallite sizes has been estimated using Scherrer's formula,

$$D = K\lambda / \beta_{2\theta} \cos\theta$$

where, the constant K is taken to be 0.9, λ the wavelength of X-ray used and $\beta_{2\theta}$ is the full width at half maximum of the diffraction patter at 2θ. The calculated average particle size of the cobalt nanoparticles has been obtained 9 nm in diameter.

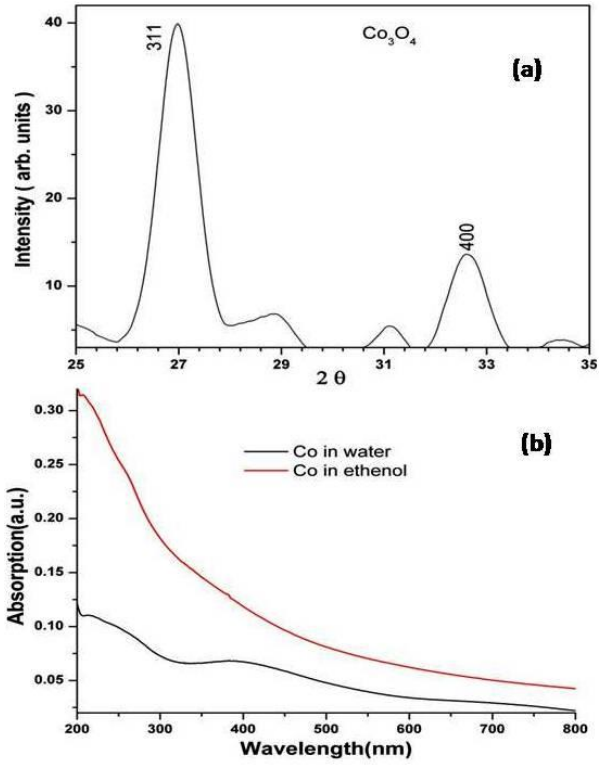

Fig. 1. (a) X-ray diffraction of as synthesized Co_3O_4 NPs and (b) UV-Visible absorption spectrum of Co_3O_4 and pure cobalt colloidal NPs.

UV-visible absorption spectroscopy

The UV-Visible absorption spectrum of as synthesized cobalt oxide (Co_3O_4) and pure cobalt (Co) colloidal solution is shown in **Fig. 1**(**b**). The absorption spectrum of cobalt oxide NPs shows a broad absorption near 400 nm is due to electronic transition between cobalt and oxygen ion, while the absorption spectrum towards shorter wavelength 200- 300 nm is due to the interband transition. UV-Visible absorption spectrum of pure cobalt colloidal NPs continuously increases towards UV resign and maximum in the range of 200-300 nm, due to SPR effect. It is already reported that metal nanoparticles show SPR effect near UV region [**19, 20**]. Chen *et al.* [**18**] have also reported that ethanol protect the oxidation of cobalt in ethanol. SPR effect is more articulate for the pure cobalt NPs rather than cobalt oxide NPs because pure cobalt NPs have more free electrons on the surface while in cobalt oxide NPs free electrons are more localized on the surface due to the oxidation.

Magnetic characterization

Magnetic behavior of nanoparticles depend on the structure of grain boundaries, the magnitude and direction of internal stress and draggling bond on surfaces, presence of any other phase and the overall size and shape of the specimen. All of these factors can be affected by the particle synthesis procedure. Typical M-H loop of as synthesized Co_3O_4 /Co NPs are shown in **Fig. 2**(**a** and **b**). Magnetic measurement of Co_3O_4 NPs has been performed using VSM at room temperature in the field range of -15k to 15k Oe. Co_3O_4 NPs show ferromagnetic character with coercivity ~67 Oe and saturation magnetization ~ 0.35 emu/gm. Hysteresis loop of pure Co NPs has been measured in the field range of -5000 to 5000 Oe with coercivity ~42 Oe and saturation magnetization ~ 0.45 emu/gm. Pure cobalt NPs show weak magnetization due to dead layer or canted surface spin on surfaces.

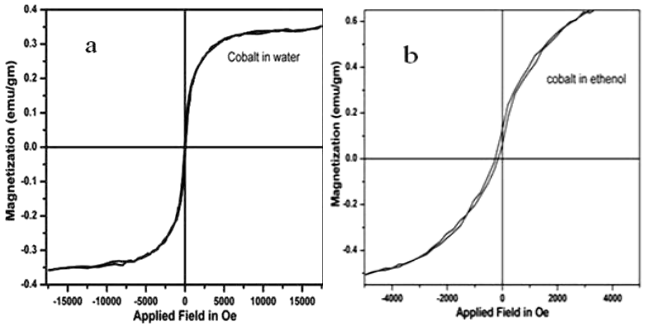

Fig. 2. Hysteresis loop of as synthesized Co_3O_4 and pure cobalt NPs (a) shows hysteresis loop of Co_3O_4 NPs and (b) shows hysteresis loop of pure cobalt NPs.

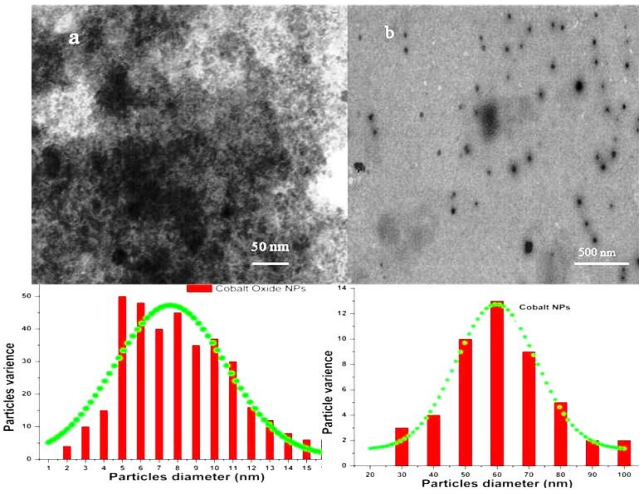

Fig. 3. TEM image of as synthesized Co_3O_4 and pure cobalt NPs (a) shows TEM image of Co_3O_4 NPs and (b) shows TEM image of pure cobalt NPs.

TEM analysis

The colloidal solution of as synthesized cobalt/cobalt oxide NPs has been dried at 60 °C for 10 minute on carbon coated cupper grid and then placed for image processing. TEM images of as synthesized cobalt oxide and pure cobalt NPs are shown in **Fig. 3**(**a** and **b**). **Fig. 3**(**a**) depicts the TEM image of cobalt oxide NPs on 50 nm bar scale. The average particle size has been found around 5-15 nm. **Fig. 3**(**b**) shows TEM image of pure cobalt NPs synthesized in ethanol on the bar scale of 0.5 μm. The average particle size of pure cobalt NPs has been found around 60-80 nm in spherical shape. Pure cobalt NPs have larger particle size

due to ageing effect between pure cobalt NPs. Ageing takes place because of the magnetic dipole attraction.

Application

Now-a-days nanomaterials and nanoparticles have received considerable attention due to their physical nature and uses in modern sciences and technology. Thus before its wide uses in our environment and system, we must know its possible impacts on our environment and it's organisms. Present study has been carried out to know the possible harmful effects of nanoparticles on plant genetic material for which AMI and chromosomal aberration assay have considered. The area of nanomaterial toxicology has already been highlighted [**21-24**].

Table 1. Effect of nanoparticles on AMI % (Active mitotic index) of *Sesbania cannabina*.

Treatment	Total no. of cells observed	No. of dividing cells	AMI (%)
Control	600	95	15.83
Ethanol	617	89	14.42
Nano-cobalt	519	67	12.90
Nano-cobalt oxide	522	61	11.68

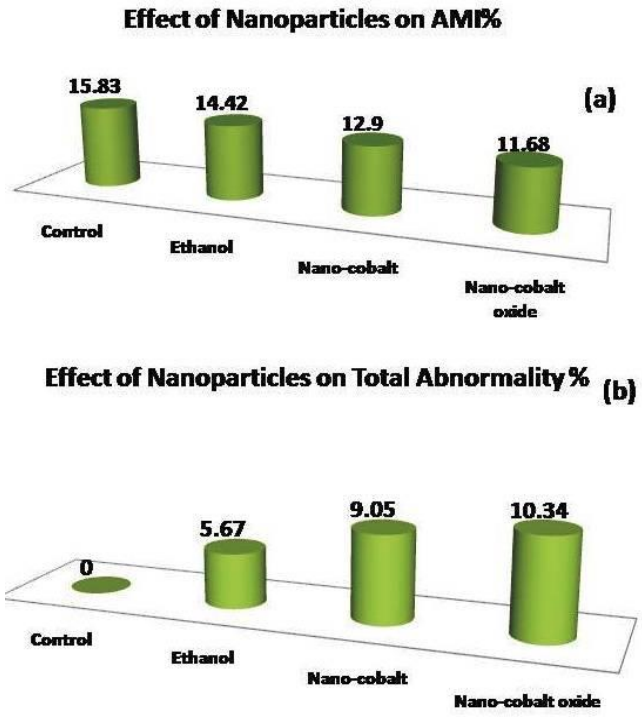

Fig. 4. (a) A comparative account on effect of nanoparticles on AMI % of *sesbania cannabina* and (b) comparative account on effect of nanoparticles on total abnormality % of *sesbania cannabina.*

Effect of cobalt nanoparticle on AMI of sesbania cannabina

The active mitotic index (AMI) % at different treated sets has been represented in **Table 1** and compared in **Fig. 4**(**a**). The highest AMI % is observed in case of control set (15.83), which decreased up to 11.68 % in case of nano-cobalt oxide treated set. Ethanol treated set exhibited value slightly lower than control (14.42). Thus from AMI % it is clear that nano-cobalt oxide is more toxic than nano-cobalt and causes a significant reduction in AMI %.

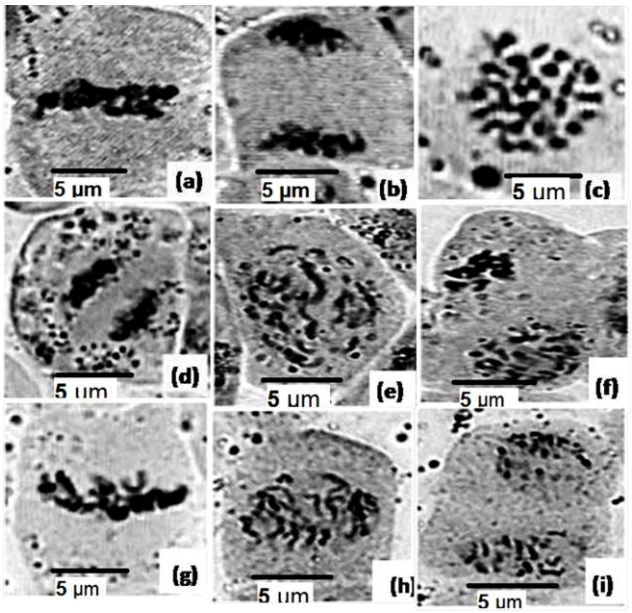

Fig. 5. (a). Normal metaphase (2n=24) (b) normal anaphase (24:24) (c) scattering at metaphase I at nano cobalt oxide treatment (d) unorientation at anaphase I at nano cobalt oxide treatment (e) Fragmentation at metaphase I at nano cobalt treatment (f) unequal separation at anaphase I at nano cobalt oxide treatment (g) precocious movement at metaphase I at nano cobalt oxide treatment (h) spindle dysfunctioning at metaphase I at nano cobalt oxide treatment and (i) scattering at anaphase I at nano cobalt oxide treatment.

Effect of cobalt-nanoparticles on meiotic division of sesbania cannabina

The mitotoxic effects of cobalt-nanoparticles on root meristmatic cells of *sesbania cannabina* were estimated on the basis of total abnormality percentages. Percentages of different types of chromosomal aberration at different treatment sets have been shown in **Table 2** and a total abnormality percentage at different treatment sets has been compared in **Fig. 4**(**b**)). Control seeds have shown a normal mitotic behavior (**Fig. 5**(**a, b**)). While ethanol and nanoparticles treated root tips show various types of chromosomal aberration in different frequencies. The Sesbania pea root tips treated with ethanol, nano-cobalt and nano-cobalt oxide solution have shown various chromosomal abnormalities (**Fig. 5**(**c-i**)), such as metaphasic plate distortion, unorientation at metaphase, breaking of chromosomes, fragmentation, spindle dysfunctioning, stickiness, scattering, precocious movement at metaphase and bridge, unequal separation, multiple bridge, fragmentation, scattering, laggard and unorientation at anaphase.

Among which most dominant aberrations are metaphasic plate distortion, fragmentation at metaphase, scattering at metaphase, bridges at anaphase and unequal separation at anaphase. The total abnormality % has been found to be highest (10.34%) in the case of nano-cobalt oxide treatment set while lowest (5.67%) in case of ethanol treated set. It is observed from **Table 2** that the highest types of chromosomal variation have been observed in case

of nano-cobalt treated set while it was lowest in case of nano-cobalt oxide treated set. The most dominant

Table 2. Effect of nanoparticles on meiotic division of *Sesbania cannabina*.

	Total no. of cells observed	No. of dividing cells	No. of abnormally dividing cells	Metaphasic abnormality %								Anaphasic abnormality %							Total abnormality %
				Pl Dis	Un	Bre	Fr	Spin	St	Sc	Pr	Br	Une	MBr	Fr	Sc	Lg	Un	
Control	600	95	-	-	-	-	-	-	-	-	-	-	-	-	-	-	-	-	-
Ethanol	617	89	35	0.48	0.16	-	0.32	0.81	-	0.81	0.32	0.64	-	-	0.64	0.64	0.16	0.64	5.67
nano-cobalt	519	67	47	1.73	0.38	0.38	1.73	1.15	0.57	0.38	-	0.57	0.77	0.57	0.57	-	-	-	9.05
nano-cobalt oxide	522	61	54	1.91	-	-	2.68	-	-	1.14	0.19	1.63	1.34	-	-	0.95	0.57	-	10.34

chromosomal aberrations are fragmentation at metaphase (2.68 %), metaphasic plate distortion (1.91 %), bridges at anaphase (1.53 %) and unequal separation at anaphase (1.34%). The percentage of different types of chromosomal aberrations has been shown in **Table 2** and total abnormality % at different treated sets compared in **Fig. 4(b)**.

Here, we have found that cobalt and cobalt oxide nanoparticles have mitotoxic and genotoxic effects on *sesbania cannabina* and it causes reduction in AMI and causes various types of chromosomal aberrations. It has been found that nano-cobalt oxide is more chromotoxic and mitodepressive than nano-cobalt. The reduction in AMI % may be due to slower progression of cells from S (DNA synthesis) phase to M (mitosis) phase of the cell cycle or due to effect of treatment of nanoparticles on microtubules. Similar chromotoxic effects of nanoparticles were also reported working on mammalian cell lines, suggesting that the nanoparticles might have penetrated sub cellular structures such as the mitochondria and nucleus causing uncoupling of respiration and increased oxidative stress [**25-28**].

The breaking of chromatids represents the DNA double strand breaks that may not have undergone through G2 repair. Any such irreversible DNA damages will lead to the chromosomal aberrations. Irreversible DNA damage would be produced whenever the trapped cleavable complex collides with a replication fork, independently of whether it is euchromatic or heterochromatic regions of the chromosomes which are being replicated [**29**]. Precocious movement of chromosomes observed might have occurred due to disturbed homology for chromosome pairing, disturbed spindle mechanism or inactivation of spindle mechanism [**30**] Laggards in the present study have been attributed to delayed terminalisation and/or failures of chromosomal movement following spindle fibre discrepancies. The fragments which appeared on the breakage of bridges, as a result of spindle fibres functioning to pull the chromosome towards poles, formed laggards [**31**]. Sticky chromosomes may be resulted from defective functioning of one or two types of specific non-histone proteins, involved in the chromosome organization which is needed for chromatid separation and segregation. Chromosomal stickiness may also be due to disturbance in nucleic acid metabolism in cells [**32**]. Unorientation at metaphase and scattering of chromosomes may be due to either the inhibition of spindle formation or the destruction of spindle fibres formed. Bridge formation may occur due to the failure of chiasmata in a bivalent to terminalize and the chromosome stretched between the poles. Single and multiple chromosome bridges may be due to the occurrence of dicentric chromosomes formed as a result of breakage fusion bridge cycles. The high frequency of mitotic abnormalities such as metaphasic plate distortion, fragmentation of chromosomes etc induced by nano-cobalt primarily reflects its effects on mitotic spindles, altering the orientation of chromosomes at various stages of the cell cycle. Impairment of mitotic spindle function is probably due to the interaction of nanoparticles with tubulin-SH group. The induction of chromosomal breaking by nano-cobalt indicates the clastogenic potential of the test chemical, which may lead to a loss of genetic material and these have been regarded as an indication of mutagenicity of the inducers.

The results of this study indicate the mitotoxic and chromotoxic effects of nano-cobalt and nano-cobalt oxide in plant system. It has been found that mitotoxic and chromotoxic impact of smaller nanoparticles is more profound than larger particles, because smaller particles may diffuse inside cell easily rather than larger particles. The effect of Cobalt oxide NPs with diameter 7-8 nm showed higher toxicity than pure cobalt NPs having diameter 60 nm.

Interaction of cobalt/cobalt oxide nanoparticle with DNA

It has been shown that nanoparticles strongly interacts with cell membranes, either adsorbing onto or compromising the membrane integrity to result in the formation of holes, with the resulting morphology depending on the nanoparticle size and surface charge [**33**]. Greater surface area per mass renders NPs more biologically active than larger-sized particles of the identical chemistry, and that particle surface area and number appear to be better predictors for NPs-induced inflammatory and oxidative stress responses [**34**]. Size dependent cellular interaction and cytotoxicity has been studied and confirmed that smaller nanoparticle produces more oxidative stress, ROS generation and DNA damage than micron sized particles [**35-36**].

Diffusion of NPs in cell also depends on highly reactive surfaces, permeability of the cellular and nuclear membranes. The oxidative stress, ROS generation and DNA damaging ability of Co_3O_4 NPs has been studied

which induce genotoxicity in human leukocytes [**37**]. Cobalt is able to cause a rapid induction of ROS if supplied in the form of Co_3O_4-NPs rather than as cobalt ions, cobalt also oxidizes proteins and cause oxidative DNA damage [**38-41**].

Double stranded DNA is highly negatively charged, having a net charge of $^{-}$2e per base pair which leads to a linear charge of -e every 0.17 nm or, equivalently, to an average surface charge density σDNA = -1.0 e nm^{-2} . The DNA and cobalt/cobalt oxide NPs may interact via electrostatic and Van der Waals forces [**42**].

It has been already reported that transition metal ions (cobalt, iron) released from their nano-particles [**43**]. Exposure to some types of nanoparticles induces oxidative stress in cells, and activation of oxidative stress-responsive transcription factors. It is generally accepted that oxidative stress eventually causes DNA damage, which plays an important role in the development of carcinogenesis [**44**]. Free radicals are atoms or molecules that contain one or more unpaired electrons and are, in this sense, "free". This makes many free radicals highly reactive, i.e. they have a strong tendency to form pairs to counteract the labile unpaired condition. To this end, the free radicals gain electrons from any available donor or donate an electron to a suitable acceptor, which in turn becomes modified into a secondary free radical. This chain reaction can cause biological damage. The ions of cobalt have potential to cause the conversion of cellular oxygen metabolic products such as H_2O_2 and superoxide anions to hydroxyl radicals ($^{\cdot}$OH), which is one of the primary DNA damaging species.

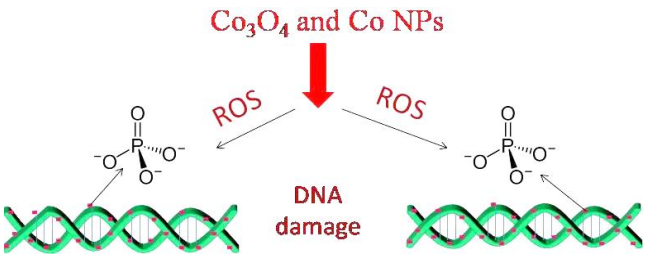

Fig. 6. Systematic pathway that Co_2O_3 and Co NPs may induce DNA damage. Co_2O_3 and Co NPs generates reactive oxygen species (ROS) by Fenton reaction. ROS react with negative charge of DNA due to phosphate. The interaction of ROS and Phosphate causes DNA damage.

The generated ROS directly react with phosphate of DNA which is negatively charged and causes DNA damage, as shown in **Fig. 6**. In the present study average particle size of cobalt oxide is 7-8 nm, while pure cobalt NPs is 60 nm. Since cobalt oxide NPs have 10- fold smaller than cobalt NPs this may be motivation to increased toxicity of Co_3O_4 NPs. This result is justified in our experiment. Oxidative stress is considered to be an important mechanism for particle-induced health effects.
The general mechanism of oxygen activation by such metal ions is provided by Fenton/Haber–Weiss and autoxidation reactions, in which molecular oxygen and its partially reduced forms superoxide O_2^- and H_2O_2 serve as substrates. Reactions (1) and (2) present conversion of H_2O_2 into hydroxyl radical (OH^-) via the oxidation of a metal cation (metal species serves as a reducing agent) [**45, 46**].

$$M^{n++} + H_2O_2 \rightarrow M^{(n+1)+} + OH^- + OH \text{ (Fentonreaction)} \quad (1)$$

The redox cycling of the metal cation is maintained by reduction with O_2.

$$M(n+1)+ + O_2{-}\cdot \rightarrow Mn+ + O_2 \quad (2)$$

The balance of these two reactions is:

$$H_2O_2 + O_2^- \rightarrow O_2 + OH^- + {}^{\cdot}OH \text{ (Haber–Weiss reaction)} \quad (3)$$

where, Mn^+ serves as cobalt cation.

Conclusion

Thus the present study concludes the mitotoxic and chromotoxic behavior of ethanol, cobalt and cobalt oxide NPs in plant system. It has been found that mitotoxic and chromotoxic impact of smaller nanoparticles are much impressive than larger particles. Cobalt oxide NPs with diameter 7-8 nm shows more toxic effect than pure cobalt NPs having diameter 60 nm, since diffusion of smaller NPs in side cell may takes place easily rather than larger particles. Here, we have seen that cobalt and cobalt oxide NPs can readily inter inside cell and induces cytogenetic effect in plant cell. Therefore, attention should be taken very carefully for the application of cobalt and cobalt oxide NPs in biological application such as MRI contrast image and drug delivery. However, toxicity of magnetic nanoparticles can be reduced or modulated by proper coating of biocompatible materials on their surfaces. Conversely, the toxicity can be exploited for the other applications such as cancer treatment. Here, we have discussed possible mechanism for interaction of magnetic NPs with DNA and ROS generation which causes different chromosomal aberration.

Acknowledgements
Authors are thankful to Dr. A. K. Sinha and Dr. Arvind Srivastav RRCAT Indore for X-ray diffraction and TEM characterization. B. K. Pandey also thankful to CSIR-New Delhi for financial support. Authors are also thankful to Sunn Hemp Research Station, Pratapgarh, India for providing seeds of *Sesbania cannabina*.

Reference

1. Pankhurst, Q. A.; Connolly, J.; Jones, S. K. ; Dobson, J. ; *J. Phys. D: Appl. Phys*. **2003**, *36*,167.
DOI: PII: S0022-3727(03)40035-1
2. Patra H. K.; Khaliq N. U.; Romu T.; Wiechec E.; Borga M.; Turner A. P. F.; Tiwari A.; *Advanced Healthcare Materials*; **2014**, *3*, 4, 526.
DOI: 10.1002/adhm.201300225
3. Yon, H.; Na, B.; Song, I. C.; Hyeon, T. ; *Adv Mater*. **2009**, *21*, 2133.
DOI: 10.1002/adma.200802366
4. Fortin, J. P.; Wilhelm, C.; Servais, J.; Christine, M.; Bacri, J. C.; Gazeau, F.; *J. Am. Chem. Soc*. **2007**, *129*, 2628.
DOI: 10.1021/ja067457
5. Veiseh, O.; Gunn, J. W.; Zhang, M.; *Adv Drug Deliv Rev*. **2010**, *62*, 284.
DOI: 10.1016/j.addr.2009.11.002.
6. Leroux, J. C.; *Nat. Nanotechnol*. **2007**, *2*, 679.
DOI: 10.1038/nnano.2007.339
7. Dobson, J.; *Gen. Ther*. **2006**, *13*, 283.
DOI: 10.1038/sj.gt.3302720
8. Xu, C.; Xu, K.; Gu, H.; Zhong, X.; Guo, Z.; Zheng, R.; *J. Am. Chem. Soc*. **2004**,*126*, 3392.
DOI: 10.1021/ja031776d

9. Mrinmoy, D.; Partha, S.; Ghosh; Vincent, M.; Rotello, *Adv. Mater.***2008**, *20*, 4225.
DOI: 10.1002/adma.200703183
10. Zhang, X.; Chan, K. Y.; *J. Mater. Chem*. **2008**, *12*, 1203.
DOI: 10.1039/B109223E
11. Pandey, B. K. ; Shahi, A. K. ; Swarnkar, R. K. ; Gopal, R.; *Sci. of Adv. Mat*. **2012, *4,*** 537.
DOI: 10.1166/sam.2012.1315
12. Zeng,H.; Cai,W.; Liu,P.; Xu,X.; Zhou,H.; Klingshirn,C.; Kalt.H. *ACS Nano*. **2008**, *2*, 166.
DOI: 10.1021/nn800353q
13. Singh, S. C. ; Gopal, R. ; Phy. E. **2010**, *114*, 9277.
DOI: 10.1016/j.physe.2007.08.155
14. Singh, S. C.; Mishra, S. K.; Srivastava, R. K.; Gopal, R.; *J. Phys. Chem. C*. **2010**, *114*, 17374.
DOI: 10.1021/jp1018907
15. William, F. G.; *Mutation Research*, **1999,** *426*,107.
DOI: 10.1016/S0027-5107(99)00050-0
16. Satyavani, K.; Gurudeeban, S.; Ramanathan, T.; Balasubramanian, T.; *J. Nanosci. Nanotechnol.*; **2011**, *1*, 95.
DOI: 10.1186/1477-3155-9-43
17. Kumar, G.; Srivastava, N.; *Chromos Botany*, **2011**, *6*, 29.
DOI: 10.3199/iscb.6.29
18. Kumar, G.; Srivastava, N.; *Electronic, J. of Plant Breeding*, **2011**,*54*, 228.
DOI: http://ejplantbreeding.com
19. Chen, G. X.; Hong, M. H.; Lan, B. ; Wang, Z. B.; Lu, Y. F.; Chong, T. C.; *Appli. Sur. Sci*. **2004**,*228*, 169.
DOI: 10.1016/j.apsusc.2004.01.007
20. Singh, M. K.; Agarwal, A.; Gopal, R.; Swarnkar, R. K.; Kotnala, R. K. ; *J. Mater. Chem*. **2011**, *21*, 11074.
DOI: 10.1039/C1JM12320C
21. Uboldi, C.; Giudetti, G.; Broggi, F. ; Gilliland, D. ; Ponti, J. ; Franc¸ O.; Rossi, F.; *Mutat. Res.* **2012,** *745*, 11.
DOI: 10.1016/j.mrgentox.2011.10.010
22. Schulz, M.; Lan, M. H. ; Brill, S. ; Strauss, V. ; Treumann, S.; Gröters, S.; Ravenzwaay, B. V.; Robert, L. *Mutation Research*, **2012**, *745*,51.
DOI: 10.1088/1742-6596/304/1/012061
23. Sharma, V.; Singh, P.; Pandey, A. K.; Dhawan, A.; *Mutation Research*. 2012, *745*, 84.
DOI: 10.1016/j.mrgentox.2011.12.009
24. Doak, S. H.; Manshian, B.; Jenkins, G. J. S.; Singh, N.; *Mutation Research*. **2012**,*745*, 104.
DOI: 10.1016/j.mrgentox.2011.09.013
25. Kelly, K. L.; Coronado, E.; Zhao, L.; George, C. S.; *J. Phys. Chem. B*., **2003**, *107*, 668.
DOI: 10.1021/jp026731y
26. Kumari, M.; Sudheer, S. K.; Pakrashi, S.; Mukherjee, A. ; *J. Hazard Mater*. **2011**, *90*, 613.
DOI: 10.1016/j.jhazmat.2011.03.095
27. Panda, K. K.; Mohan, V.; Achary, M.; Krishnaveni, R.; Padhi, B. K.; Sachindra, N.; Surendra, N.; Sarang,S.; B Panda , B.*B. Toxicol. In Vitro*. **2011**, *25*, 1097.
DOI: 10.1016/j.tiv.2011.03.008
28. Li, N.; Sioutas, C.; Cho, A.; Schmitz D.;, Mistra, C.; Sempf, J. M. *Environ, Health Perspect***. 2003**, *111*, 455.
DOI: 10.1289/ehp.6000
29. Chen, M.; Mikecz, A. V. ; *Exp. Cell Res*. **2005**,*305*, 51.
DOI: 10.1016/j.yexcr.2004.12.021
30. Anita, K.; Patlolla, Berry, A.; LaBethani, M.; Paul, B. T.; Int. *J. Environ. Res. Public Health.* **2012**, *9*, 1649.
DOI: 10.3390/ijerph9051649.
31. Agarwal, R.; Ansari, M. Y. K.; *Cytol. Genet.* **2001**, *2*, 129.
DOI: 10.1007/978-1-4615-1305-6_23
32. Kumar, G.; Gupta, P.; *Turk J. Biol.* **2009**, *123*.
DOI: 10.3906/biy-0807-29
33. Paillusson,F.; Dahirel,V.; Jardat,M.; Victor,G.M.; Barbi,M;. *Phys. Chem. Chem. Phys.* **2007**, *7*, 3716.
DOI: 10.1039/C1CP20324J
34. Oberdörster,G.; Oberdörster, E.; Oberdörste, J.*; Biomaterials*; **2005,** *113*, 823.
DOI: 10.1016/j.biomaterials
35. Carlson,C.; Hussain,S. M.; Schrand,A. M.; Braydich-Stolle,L. K.; Hess,K.L.; Jones,R. L.; Schlager,J.J.*; Chem. Res. Toxicol***, 2008,** *112***,** 13608.
DOI: 10.1021/tx300065v
36. Papageorgiou, I.; Brown, C.; Schins,R.; Singh,S.; Newson,R.; Davis, S.; Fisher,J.; Ingham,E.; Case, C.P.; *Biomaterials*, **2007**, *28*, 2946.
DOI: 10.1016/j.mrgentox.2010.01.012
37. Colognato,R.; Bonelli ,A.; Ponti,J.; Farina, M.; Bergamaschi ,E.; Sabbioni,E.; Migliore,L.; *Mutagenesis*. **2008**, *23*, 377.
DOI: 10.1093/mutage/gen024
38. Alarifi,S.; Ali,D.; Suliman, A. O. Y,; Ahamed, M,; Siddiqui, M. A.; Khedhairy, A.; *International Journal of Nanomedicine*. **2013**, *8*,189.
DOI: 10.2147/IJN.S37924
39. Petit, A.; Mwale, F,; Tkaczyk,C.; Antoniou, J.; Zukor, D. J.; Huk O. L.; *Biomaterials.*, **2005**, *26*, 4416.
DOI: 10.1016/j.biomaterials.2004.11.019
40. Boeck, M.D.; Lison,D.; Volders, M. K.; *Carcinogenesis*, **1998**, *19*, 2021.
DOI: 10.1093/carcin/19.11.2021
41. Papis,E.; Rossi, F.; Raspanti, M.; Donne, I. D.; Colombo, G.; Milzani, A.; Bernardini, G.; Gornati, R.; *Toxicology Letters* **2009**,189.
DOI: 10.1016/j.toxlet.2009.06.851
42. Paillusson, F.; Dahirel, V.; Jardat, M.; Victor, J. M.; Barbi, M.; *Chem. Chem. Phys*. **2011**,13,12603.
DOI: 10.1039/c1cp20324j.
43. Singh, N.; Manshian, B.; Jenkins, G.K.; Griffiths, S. M.; Williams, P. M.; Maffeis, T. G.; Wright, C. J.; Doak, S. H.; *Biomaterials.* **2009**, *30*, 3891.
DOI: 10.1016/j.biomaterials.2009.04.009
44. Rafael,G. B.; Marina, G. P.; Calle, E.; Casado, J.; *Chem. Res. Toxicol*. **2012**, *25*, 1402.
DOI: 10.1021/tx200513t
45. Valko, M.; Morris, H.; Cronin, M.T.; *Current Medicinal Chemistry*. **2005**, *12*, 1161.
DOI: 10.2174/0929867053764635
46. Bal, W.; Kasprzak, K. S.; *Toxicology Letters*, **2002**, *127*, 55**.**
DOI: 10.1016/S0378-4274(01)00483-0